

# The relative effects of Ca and Mg ions on MSC osteogenesis in the surface modification of microrough Ti implants

This article was published in the following Dove Press journal:  
*International Journal of Nanomedicine*

Jin-Woo Park<sup>1</sup>  
Takao Hanawa<sup>2</sup>  
Jong-Hyuk Chung<sup>3</sup>

<sup>1</sup>Department of Periodontology, School of Dentistry, Kyungpook National University, Daegu 41940, Republic of Korea; <sup>2</sup>Department of Metallic Biomaterials, Institute of Biomaterials and Bioengineering, Tokyo Medical and Dental University, Tokyo 101-0062, Japan; <sup>3</sup>Department of Periodontology, School of Dentistry, Kyung Hee University, Seoul, Republic of Korea

**Purpose:** Calcium (Ca) and magnesium (Mg) ions have been used as promising bioactive ions in the surface chemistry modification of titanium (Ti) bone implants to increase bone regeneration capacity. However, it is not clear which (Ca or Mg) plays the more important role in the early osteogenic differentiation of mesenchymal stem cells (MSCs) when applied to the surface of commercially available microstructured Ti implants. This study investigated the relative effect of these two ions on the early osteogenic functionality of primary mouse bone marrow MSCs in order to obtain insights into the surface design of Ti implants with enhanced early osteogenic capacity.

**Methods and results:** Wet chemical treatment was performed to modify a microrough Ti implant surface using Ca or Mg ions. Both the Ca and Mg-incorporated surfaces accelerated early cellular events and the subsequent osteogenic differentiation of MSCs compared with an unmodified microrough Ti surface. Surface Mg modification exhibited a more potent osteoblast differentiation-promoting effect than the Ca modification. Surface Mg incorporation markedly inhibited the phosphorylation of  $\beta$ -catenin.

**Conclusion:** These results indicate that alteration of the surface chemistry of microstructured Ti implants by wet chemical treatment with Mg ions exerts a more effect on promoting the early osteogenic differentiation of MSCs than Ca ions by enhancing early cellular functions, including focal adhesion development and stabilization of intracellular  $\beta$ -catenin.

**Keywords:** divalent cations, surface chemistry, nanotopography, bone implant

## Introduction

The alteration of surface chemistry using bioactive ions and nano-topographical modification is believed to be a promising approach to the development of load-bearing titanium (Ti) bone implants that have enhanced early bone regeneration capacity.<sup>1-5</sup> Ca and Mg ions are basic components of hard tissue and have been employed in the fabrication of bone replacement materials and also in the surface modification of metallic implants, including permanent Ti oral implants.<sup>2,3,6-8</sup> These two ions are representative divalent cations that promote the early cellular events of bone-forming cells, such as attachment and spreading. This results in enhanced osteoblastic differentiation and ultimately, early bone healing of Ti implants, when employed as a surface modification.<sup>2,3,6-10</sup>

Although studies have demonstrated the beneficial effects of surface chemistry alteration using Ca or Mg in early bone apposition of implants,<sup>2,3,6-10</sup> it is still unclear which ion exerts the dominant role in the promotion of early osteogenic

Correspondence: Jin-Woo Park  
School of Dentistry, Kyungpook National University, 2177 Dalgubeol-daero, Jung-Gu, Daegu 41940, Republic of Korea  
Tel +82 53 257 6883  
Fax +82 53 257 6883  
Email jinwoo@knu.ac.kr

differentiation of mesenchymal stem cells (MSCs) and implant osseointegration when employed in the surface chemistry alteration of microstructured Ti oral implants. Thus, this study aimed to evaluate which ion, Ca or Mg, is more effective in enhancing the early osteogenic functions of MSCs in surface chemistry in microstructured Ti implants. Our previous studies have demonstrated that a simple wet chemical treatment is highly effective for the delivery of various bioactive ions into the surface of microstructured Ti implants without altering underlying original micron- and submicron-scale surface topography.<sup>5,7,9,10</sup>

In this study, we incorporated Ca or Mg ions into a commercially available grit-blasted microrough Ti implant surface by wet chemical treatment, then investigated the relative effects of these two ions on the early and later stages of osteogenesis-related cellular functions using mouse bone marrow-derived MSCs to provide insight into the future development of oral implants with enhanced early bone regeneration capacity.

## Materials and methods

### Sample preparation

Commercially pure Ti disks (ASTM grade 4, 15 mm in diameter and 2 mm thick) were subjected to grit-blasting using resorbable blast media (hydroxyapatite particles) to prepare a microrough surface of a commercially available Ti oral implant. After grit-blasting, Ti samples were cleaned in nitric acid (RBM group). Surface modification was then carried out so as to produce Ca- or Mg-containing nanostructures in the RBM samples by wet chemical treatment according to a method described previously.<sup>9,10</sup> Briefly, RBM samples were treated hydrothermally using a mixed solution of NaOH and CaO (Ca group) or MgO (Mg group) at 160°C for 2 hrs, and then thoroughly cleaned using deionized water and dried.

### Surface characterization

Surface morphology of the investigated samples was evaluated by field emission-scanning electron microscopy (FE-SEM; S-4800, Hitachi, Tokyo, Japan). The micron-scale surface roughness value was measured by non-contact optical profilometry (WYKO NT 2000, Veeco, Woodbury, NY, USA) over a 320  $\mu\text{m}$   $\times$  240  $\mu\text{m}$  area (n=5). The crystalline structure and chemical composition of the surface layer of the investigated samples were evaluated by thin-film X-ray diffractometry (XRD; X'Pert-APD, Philips, Almelo, Netherlands) and X-ray

photoelectron spectroscopy (XPS; K-Alpha, Thermo Scientific, East Grinstead, UK).

The surface hydrophilicity of the samples was evaluated using an automatic contact angle meter (Phoenix 3000; Surface Electro Optics, Seoul, Korea) by measuring the static contact angle (at 10 and 30 s) of one drop of deionized water (5  $\mu\text{L}$ ) under normal room conditions (n=7). The surface energy of the investigated samples was automatically calculated following the Girifalco-Good-Fowkes-Young rule using the manufacturer's software (Surface Electro Optics) according to a previously described method.<sup>11</sup>

Ca and Mg ions release from the treated samples were evaluated by inductively coupled plasma-atomic emission spectroscopy (ICP-AES; Optima 3000, Perkin Elmer, Norwalk, CT, USA) under two different incubation conditions, ie, a static mode without any shaking and a dynamic mode with gentle shaking of the samples (at 50 rpm). Each Ca and Mg samples were soaked in 1 mL of 0.9% NaCl solution in a sealed bottle at 37°C (n=5). The saline solution was retrieved and replaced with new solution at the indicated immersion time-points. The concentration of Ca and Mg ions released from the Ca and Mg samples into the saline solution was measured after 4 hrs, and also 1, 2, 4 and 8 days of immersion.

### Cell culture

Primary bone marrow MSCs were isolated from the bone marrow of the tibia and femur of 6-week-old mice. We used cell stock obtained from previous experiments underwent according to the protocol approved by the Institutional Animal Care and Use Committee of Kyungpook National University, Daegu, Korea [approval no. KNU 2011-96]. Korean national regulations (equivalent to NIH guidelines; NIH Publication no. 85-23 Rev. 1985) for the care and use of laboratory animals were observed. Cells were maintained in  $\alpha$ -minimum essential medium (MEM) (Gibco BRL Life Technologies, Grand Island, NY, USA) containing 10% FBS (Gibco BRL Life Technologies), 100 U/mL penicillin (Keunhwa Pharmaceutical, Seoul, Korea), and 100 U/mL streptomycin (Donga Pharmaceutical, Seoul, Korea). The cells were cultured under 100% humidity and 5% CO<sub>2</sub>, at 37°C. The medium was changed every 3 days, and after the confluence, cells were digested with 0.25% trypsin/0.02% EDTA. Cells from passage 2 to 4 were used for experiments. On day 2, post-plating of the cells on the Ti samples, differentiation was induced by the addition of

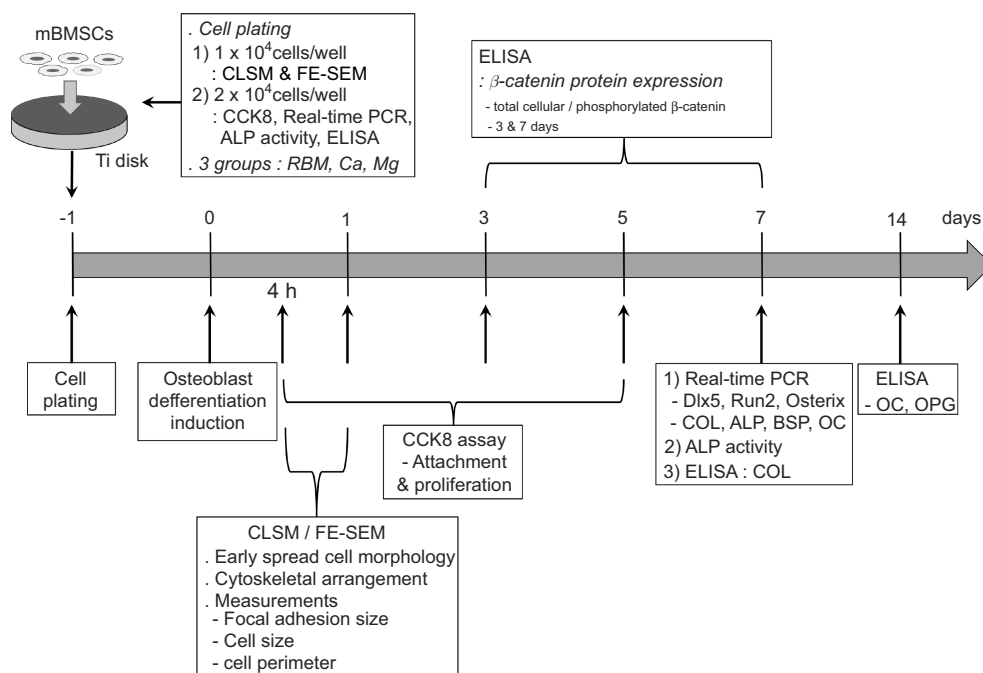


**Figure 1** Flow chart of the cell culture experimental design.

50  $\mu\text{g}$  ascorbic acid/mL and 10 mM  $\beta$ -glycerophosphate. Cell culture experimental design of this study is summarized in Figure 1.

## Evaluation of morphology of spread cells

Confocal laser scanning microscopy (CLSM) and FE-SEM observation were used to investigate the morphology, cytoskeletal arrangement and focal adhesion development in adherent MSCs on the investigated samples at 4 and 24 hrs of culture. Cells were cultured on Ti disks at an initial seeding density of  $1 \times 10^4$  cells/well. The distribution of vinculin and organization of the actin filaments of the attached MSCs on the investigated samples was evaluated by CLSM (LSM700; Carl Zeiss, Oberkochen, Germany), which were identified following the double staining of actin (green fluorescence) and vinculin (red fluorescence) using diluted monoclonal anti-vinculin (Sigma–Aldrich, St. Louis, MO, USA), goat-anti-mouse IgG (Invitrogen, Carlsbad, CA, USA), and fluorescein isothiocyanate-labeled phalloidin (Sigma–Aldrich) according to a method described previously.<sup>9</sup> For the FE-SEM observation, MSCs spread on the investigated samples were fixed with 2% glutaraldehyde and 1% osmium tetroxide, then dehydrated using an ascending series of alcohols. After critical point drying and gold–palladium coating, the cell morphologies were observed using FE-SEM.

## Determination of the cell perimeter, cell area and focal adhesion size of MSCs

Quantitative analysis of the cell area, cell perimeter and focal adhesion contact size of the MSCs on the investigated samples was performed using image analysis software (i-Solution, iMTechnology, Suwon, Korea). The perimeter and spread area of the cells were measured in 50 cells from random CSLM images (at a magnification of  $\times 200$ ) of three Ti samples at 4 and 24 hrs of culture (at an initial seeding density of  $1 \times 10^4$  cells/well). The focal adhesion size of the spread cells was measured using magnified CLSM images according to the method described elsewhere.<sup>9,12,13</sup>

## Cell attachment and proliferation assay

Cells were cultured on Ti disks in 24-well culture plates at an initial seeding density of  $2 \times 10^4$  cells/well for the evaluation of the initial cell attachment and proliferation. The initial cell attachment was evaluated after 4 hrs of culture. Cells were cultured for 1, 3 and 5 days for cellular proliferation assay. Cell attachment and proliferation were assessed using a cell counting kit-8 (Dojindo Molecular Technologies, Tokyo, Japan) in accordance with the manufacturer's instructions according to a previously described method ( $n=7$  per group).<sup>9</sup> The absorbance value was measured at 450 nm.

## Real-time PCR analysis of osteogenesis-related gene expression

The mRNA expression levels of critical transcription factor genes regulating osteogenic differentiation (Dlx5, Runx2 and osterix) and osteoblast phenotype genes [type I collagen (COL), ALP, bone sialoprotein (BSP) and osteocalcin (OC)] in MSCs grown on the investigated samples were evaluated at 7 days of culture (at an initial seeding density of  $2 \times 10^4$  cells/well). RNA was extracted from the cells cultured on seven Ti disk samples per group using Trizol reagent (Invitrogen). Real-time PCR was performed as described previously<sup>9</sup> using the primers shown in Table 1. The levels of genes were expressed as fold differences in gene expression relative to the unmodified RBM surface.

### ALP activity

Total cellular ALP activity in the cell lysates was measured in 2-amino-2-methyl-1-propanol buffer, pH 10.3, at 37°C with p-nitrophenyl phosphate as the substrate at 7 days of culture at an initial seeding density of  $2 \times 10^4$  cells/well. The absorbance change at 405 nm was measured using a microplate reader (n=7 per group). Total protein was extracted from the cell lysates using a protein extraction solution (Thermo Fisher Scientific, Rockford, IL, USA) and quantified with Pierce™ BCA Protein Assay kit (Thermo Fisher Scientific) according to the manufacturer's instructions (n=5 per group). ALP activity was expressed as nanomoles of p-nitrophenol liberated per microgram of total cellular protein.

### ELISA for the detection of osteoblast-specific protein production by MSCs

The protein concentration of the osteoblast differentiation markers produced by MSCs and secreted into the cell culture media was measured with a commercially available ELISA kit. The protein concentration of early

osteoblast maturation marker secreted by MSCs was measured with a commercially available type I COL ELISA kit (Cosmo Bio, Carlsbad, CA, USA) at 7 days of culture according to the manufacturer's instructions (at an initial seeding density of  $2 \times 10^4$  cells/well). The protein concentration of terminal osteogenic differentiation markers secreted by adherent MSCs into cell culture media, ie, OC and osteoprotegerin (OPG), was measured with commercially available OC (R&D Systems, Minneapolis, MN, USA) and OPG (Abcam, Cambridge, UK) ELISA kits at 14 days of culture (at an initial seeding density of  $2 \times 10^4$  cells/well). The COL, OC and OPG protein levels in the supernatant were measured at 450 nm (n=7 per group). The data were normalized to the total protein content.

### Assessment of the total cellular and phosphorylated $\beta$ -catenin protein expression in MSCs

The protein expression level of the total cellular  $\beta$ -catenin and phosphorylated  $\beta$ -catenin (phosphorylated at Ser 45; pS45) in MSCs grown on the investigated samples was semi-quantitatively measured using a commercially available  $\beta$ -catenin ELISA kit (ab205705; Abcam) at 3 and 7 days of culture according to the manufacturer's instructions (at an initial seeding density of  $2 \times 10^4$  cells/well). The protein levels of pS45 and total  $\beta$ -catenin in the cell lysates of adherent MSCs were measured at 600 nm (n=7 per group). The data were normalized to the total protein content. The protein expression levels of pS45 and total  $\beta$ -catenin were expressed as fold differences relative to the results from an unmodified RBM surface.

### Statistical analysis

Three independent cell culture experiments were performed. Statistical analysis was performed using one-way

**Table 1** Primer sequences for real-time PCR

Target	Forward primer sequence (5'–3')	Reverse primer sequence (5'–3')
Dlx5	TGT AAC TCG CCA CAG TCA CCA G	GAA GCC GAG TTC TCC AGG TAG C
Runx2	TAA GAA GAG CCA GGC AGG TG	TGG CAG GTA CGT GTG GTA GT
Osterix	TCA CTT GCC TGC TCT GTT CC	GCG GCT GAT TGG CTT CTT CT
COL	ATC CAA CGA GAT CGA GCT CA	GGC CAA TGT CTA GTC CGA AT
ALP	CTT GAC TGT GGT TAC TGC TG	GAG CGT AAT CTA CCA TGG AG
BSP	GGA GGA GAC AAC GGA GAA GA	CCA TAC TCA ACG GTG CTG CT
OC	TGC TTG TGA CGA GGT ATC AG	GTG ACA TCC ATA CTT GCA GG
GAPDH	GGC ATT GCT CTC AAT GAC AA	TGT GAG GGA GAT GCT CAG TG

**Abbreviations:** COL, type I collagen; BSP, bone sialoprotein; OC, osteocalcin; GAPDH, glyceraldehyde-3-phosphate dehydrogenase.

ANOVA with Tukey's multiple comparison tests.  $P < 0.05$  was considered statistically significant.

## Results and discussion

### Surface characteristics of the investigated samples

Figure 2 shows the surface morphologies of the investigated samples. All of the investigated surfaces displayed an essentially identical rough surface morphology obtained by grit blasting at the micro-scale (at a magnification of  $1000\times$ ). At higher magnifications ( $\times 50,000$  and  $\times 80,000$ ), the samples exhibited a notable difference in surface morphology at the nanoscale (Figure 2). The RBM surface was relatively smooth at the nanometer level. In contrast, the wet chemical-treated samples (Ca and Mg) exhibited the formation of clearly evident surface nanostructures. There was an obvious difference in the morphology of surface nanostructures between the Ca and Mg samples. The Ca sample exhibited nodular nanostructures  $< 50$  nm in dimension, while the Mg sample surface was covered with platelet-like nanostructures with a wall thickness of approximately 10 nm (Figure 2). All of the investigated samples exhibited an identical micron-scale surface roughness value ( $R_a$  of  $1.8 \pm 0.2 \mu\text{m}$ ). Thus, wet chemical

treatment produced Ca or Mg-incorporated nanostructures without altering the typical microtopography of a grit-blasted Ti implant surface.

Figure 3A shows the results of thin-film XRD analysis of the Ca and Mg samples. In contrast to the Ca sample that displayed a crystalline structure of a Ca-containing Ti oxide layer as  $\text{CaTiO}_3$  (JCPDS #22-0153), the Mg sample did not exhibit any peaks displaying the formation of a crystalline oxide structure after the wet chemical treatment. Deconvolution of the  $\text{Mg}2p$  spectrum was further performed to verify the Mg binding state in the Ti oxide layer of the Mg sample on XPS analysis. Figure 3B shows the chemical composition of the unmodified RBM, Ca and Mg samples determined by XPS analysis. The atomic percentages of Ti, O, C, Ca and P for the unmodified RBM surface were 19%, 55.9%, 22.5%, 0.2% and 1.4%, respectively. A small amount of Ca and P found in the RBM sample was attributable to minute HA grit remnants embedded in the surface after the grit-blasting process. The atomic percentages of Ti, O, C, Ca and P for the Ca surface were 12.8%, 53.1%, 18.7%, 14.8% and 0.5%, respectively. The Mg sample had surface Mg content of 6.5%. The atomic percentage of Ti, O, C, Ca and P of the Mg surface was 23.7%, 55.8%, 13%, 0.2% and 0.1%, respectively. Minute amounts of N and Na were detected as surface

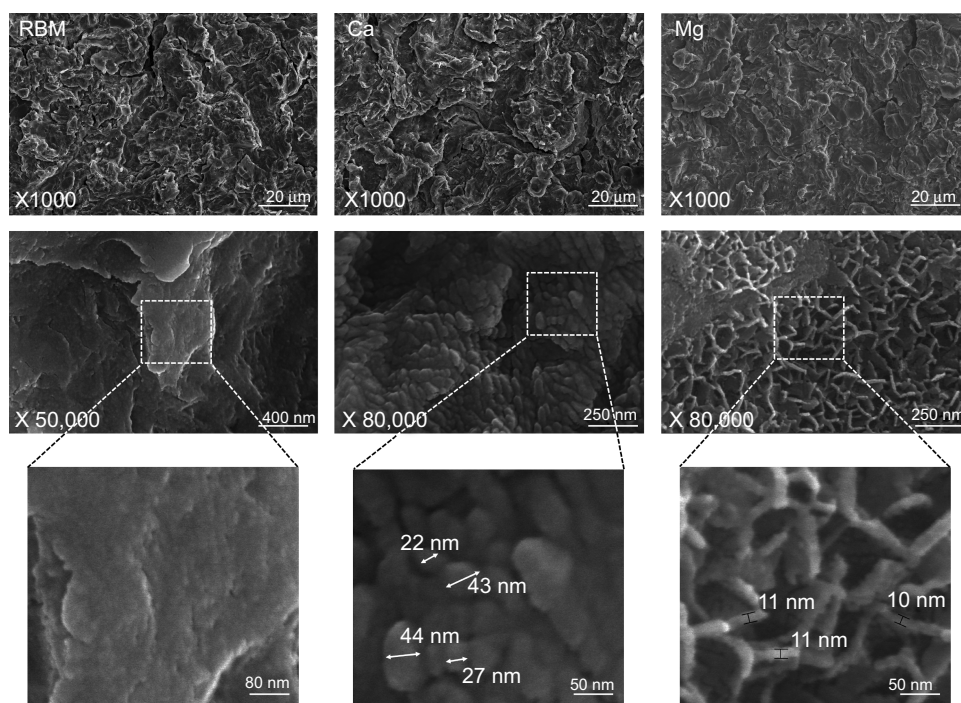


**Figure 2 (Upper)** FE-SEM images showing the micron-scale surface topography at a magnification  $\times 1000$ . **(Middle)** Nanoscale topography at magnifications  $\times 50,000$  and  $\times 80,000$ . **(Lower)** Higher magnification images showing the dimension of surface nanostructures of the unmodified RBM, Ca and Mg samples investigated samples.

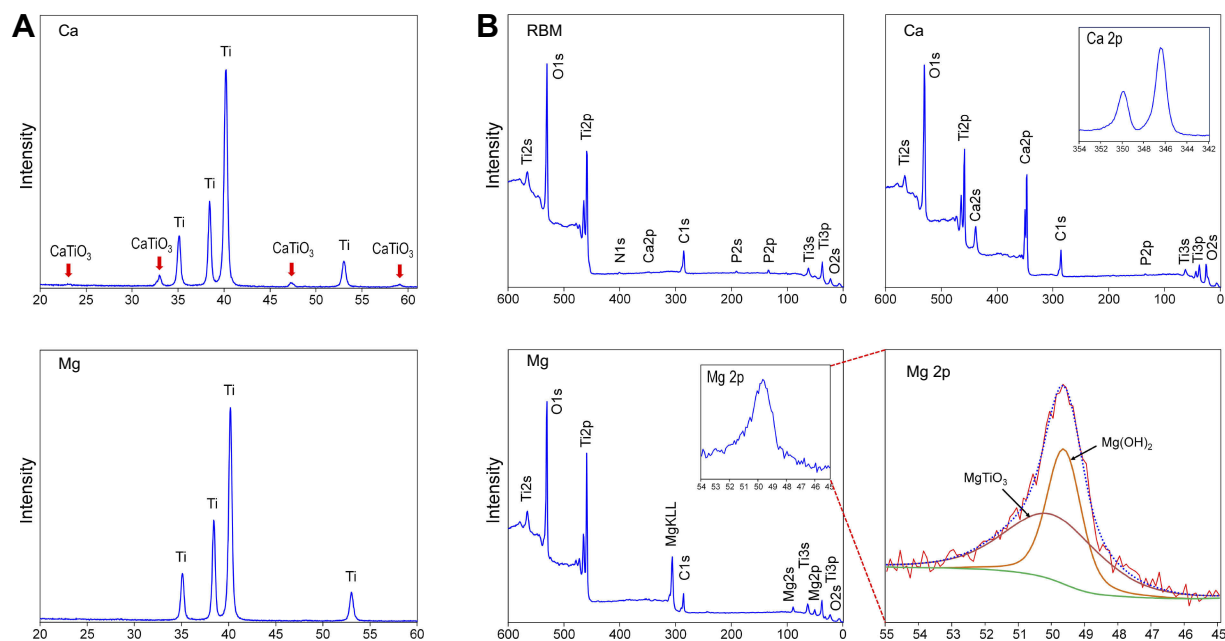


**Figure 3** (A) X-ray diffraction pattern of the Ca and Mg samples. (B) X-ray photoelectron survey spectra of the RBM, Ca and Mg samples, and the high-resolution spectrum of the Mg2p peak of the Mg sample were subjected deconvolution.

contaminants in all of the investigated samples. The Mg2p spectrum was deconvoluted into two peaks (Figure 3B). The binding energies of Mg2p in the Mg sample were 49.7 and 50.3 eV, which correspond to  $\text{Mg(OH)}_2$  and  $\text{MgTiO}_3$ .<sup>6</sup> This finding may indicate the Mg sample surface has a Mg titanate structure, but its crystallinity is too low to display peaks on XPS analysis. It appeared that the surface of the  $\text{MgTiO}_3$  layer was covered with a  $\text{Mg(OH)}_2$  layer because of the high reactivity of Mg.

Figure 4A shows the water contact angles of the investigated samples. The Mg sample displayed hydrophilic surface properties. The Mg sample exhibited a

significantly lower water contact angles than the unmodified RBM and surface Ca-modified nanostructured Ti samples ( $P < 0.05$ ). There was no difference between the RBM and Ca samples in terms of water contact angle. The surface Mg-modified Ti sample displayed a notably higher surface energy than the RBM and Ca samples ( $P < 0.05$ ; Figure 4B). It is suggested that the hydrated surface chemistry and porous platelet-like nanotopography contributed to the increased surface wettability of the Mg sample.<sup>14</sup>

Figure 5 shows the concentration of the Ca and Mg ions released from the Ca and Mg samples into saline solution as determined by ICP-AES analysis. The Ca

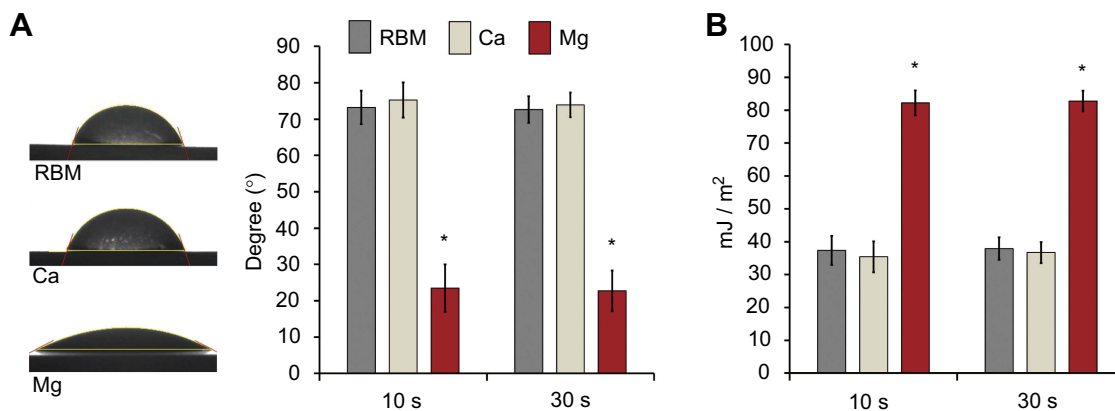


**Figure 4** (A) Water contact angles of the investigated samples measured at 10 and 30 s. (B) Surface energies of the investigated samples determined at 10 and 30 s. Data are presented as the mean  $\pm$  SD (n=7). \* $P < 0.05$  compared with the other surface.

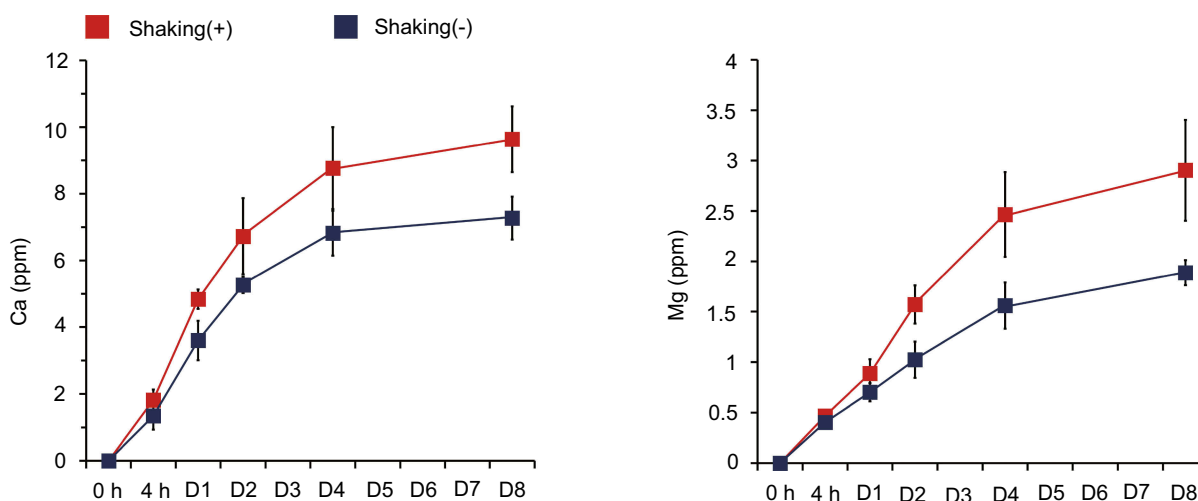


**Figure 5** Release of Ca and Mg ions from the Ca and Mg samples as determined by inductively coupled plasma-atomic emissionspectroscopy (ICP-AES) analysis. Data are presented as the mean  $\pm$  SD (n=5).

sample released a higher amount of Ca ions in the dynamic mode with gentle shaking than in the static mode. The Ca ions released from the Ca samples in the static and dynamic modes on the first day of incubation were  $3.6 \pm 0.6$  ppm and  $4.8 \pm 0.3$  ppm, respectively. The cumulative concentrations of Ca ions released from the Ca samples in the static and dynamic mode for 8 days of incubation were  $7.3 \pm 0.6$  ppm and  $9.6 \pm 1.0$  ppm, respectively. The Mg sample released a higher amount of Mg ions under the gentle shaking condition than the static condition (Figure 5). On the first day of incubation, the Mg ion concentrations in the static mode and under the gentle shaking condition were  $0.7 \pm 0.1$  ppm and  $0.89 \pm 0.14$  ppm, respectively. The total concentrations of Mg ions released from the Mg samples in the static and dynamic modes for 8 days of incubation were  $1.9 \pm 0.1$  ppm and  $2.9 \pm 0.5$  ppm, respectively. Thus, these findings suggest that in vivo ion release from the surface ion-modified Ti implants after placement in bone tissue would be much higher than under the 2D static cell culture experiment condition because of the continuous circulation that occurs in the physiological setting.

Studies have suggested that that small deviations in the extracellular Ca concentration from the physiological value directly regulate osteoblast functions.<sup>15,16</sup> It has been reported that extracellular Ca uptake by cells facilitates intracellular Ca signaling that regulates osteoblast cell fate.<sup>15,17,18</sup> Mg ions are known to activate the transient receptor potential melastatin 7/phosphoinositide 3-kinase signaling pathway and then subsequently induce the

recruitment and osteogenic differentiation of hFOB1.19 human osteoblast cells<sup>19</sup> as well as rat calvarial osteoblasts.<sup>20</sup> Studies have reported that Mg supplementation enhances focal adhesion formation, ALP activity and osteoblast gene expression in primary human osteoblasts.<sup>20,21</sup> Mg supplementation dose-dependently promotes the osteogenic differentiation and mineralization of rabbit bone marrow MSCs.<sup>22</sup> Mg coating and Mg-based alloys are suggested to have the potential to enhance the bone regeneration effect of implants.<sup>8</sup>

Thus, it may be reasonably expected that Ca and Mg ion release from the modified Ti surface increases the extracellular ion levels, which would subsequently affect the intracellular ion concentration of adherent cells on the Ti implant surfaces and as a result positively modulate the osteogenic functionality of bone-forming cells, including MSCs, through the activation of osteogenesis-related intracellular signaling. Thus, a Ti implant surface modified to have sustained Ca and Mg release would be beneficial for inducing a favorable osteogenesis outcome.

### The cell morphology and focal adhesion formation of MSCs adhering to the investigated samples

The morphologies of the bone marrow MSCs spread on the investigated surfaces evaluated by CLSM are shown in Figure 6. At 4 hrs, they displayed weak cytoplasmic extensions and focal adhesions. Surface ion-modified nanostructured Ti samples supported better cell spreading compared

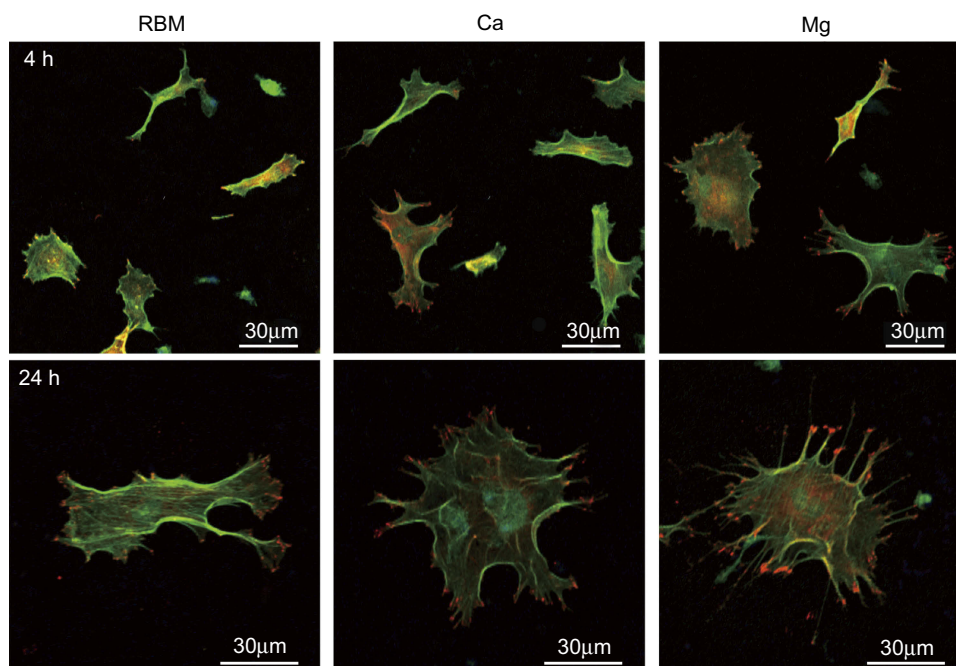


**Figure 6** Merged confocal laser scanning microscopy (CLSM) images of the spread mesenchymal stem cells (MSCs) on the investigated surfaces showing actin cytoskeleton (green) and focal adhesions (red) at 4 and 24 hrs of incubation.

with the unmodified RBM sample. Cells on the Ca and Mg samples were larger than on the RBM sample, and also displayed more cytoplasmic extensions. At 24 hrs, the MSCs on all of the investigated surfaces had entered the advanced stages of cell spreading, ie, they were larger, and had more accentuated cytoplasmic extensions and stronger focal adhesions compared with these samples at 4 hrs. However, the cells on the Ca and Mg samples exhibited

better spreading and focal adhesion formation compared with the RBM sample. Cells on the Mg surface displayed numerous filopodial attachments and markedly enhanced focal adhesions compared with the Ca and RBM surfaces.

**Figure 7** shows the FE-SEM images of the spread MSCs on the investigated samples at 4 and 24 hrs of incubation. The MSCs on the Ca and Mg samples exhibited better-spread morphology than the RBM sample, ie,

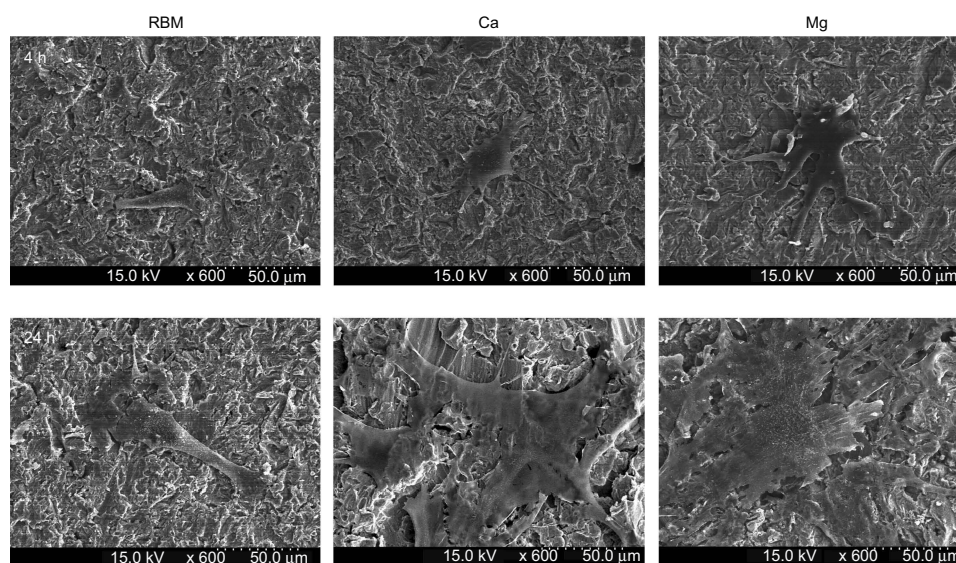


**Figure 7** Field emission-scanning electron microscopy (FE-SEM) images showing the morphology of spread mesenchymal stem cells (MSCs) on the investigated surfaces at 4 and 24 hrs of incubation.



polygonal shape cells with a larger cell body and more extensive cytoplasmic extensions.

The results of quantitative measurements of the cell size, perimeter and focal adhesion size of MSCs adhering to the investigated samples are shown in Figure 8. At 24 hrs, the spread MSCs exhibited an increased cell size and perimeter in all of the investigated samples compared these features at 4 hrs (Figure 8A). Cells on the Ca and Mg-modified nanostructured Ti sample surfaces displayed significantly increased cell area and cell perimeter at both the 4 and 24 hrs of incubation time-points compared with the unmodified RBM surface ( $P<0.05$ ; Figure 8A). At 24 hrs, the focal adhesion size was increased in the MSCs grown on the Ca and Mg samples compared with the unmodified RBM sample ( $P<0.05$ ; Figure 8B). Mg incorporation further increased the focal adhesion size of MSCs when compared with the results of Ca incorporation in the microrough Ti surface ( $P<0.05$ ; Figure 8B). Focal adhesion size was increased in the MSCs in both the Ca and Mg samples with increased incubation time, but there was no difference in focal adhesion size in the cells grown on the RBM surface between the two incubation time-points.

Studies have demonstrated that a polygonal cell shape along with a better spread morphology, ie, strong cytoplasmic extensions, accentuated filopodial attachments

and greater focal adhesions, are indicative of cells having a high osteogenic potential.<sup>9,23,24</sup> Thus, these findings suggest that modification of a microrough Ti implant surface using Ca and Mg ions is beneficial for obtaining favorable cell functions and inducing the osteogenic differentiation of MSCs during early stages of implant-bone healing.

## Cell attachment and proliferation

Surface Mg modification enhanced early cell spreading and the development of focal adhesions, but resulted in a decreased number of early attachments of MSCs. The Mg-treated surface displayed a lower level of early cell attachment (4 hrs) compared to unmodified RBM and Ca surfaces ( $P<0.05$ ; Figure 8C). This lower early attachment of MSCs on the Mg-modified surface at 4 hrs resulted in subsequent decreases in cell proliferation at 1 and 3 days ( $P<0.05$ ; Figure 8D). No differences were found in cell attachment (4 hrs) or early cell proliferation (24 hrs) between the RBM and Ca surfaces, but surface Ca modification increased the proliferation of MSCs compared to the unmodified RBM sample at 3 days ( $P<0.05$ ; Figure 8D). At 5 days, the Ca surface supported better cell proliferation compared with the RBM and Mg surfaces ( $P<0.05$ ; Figure 8D), but no difference was

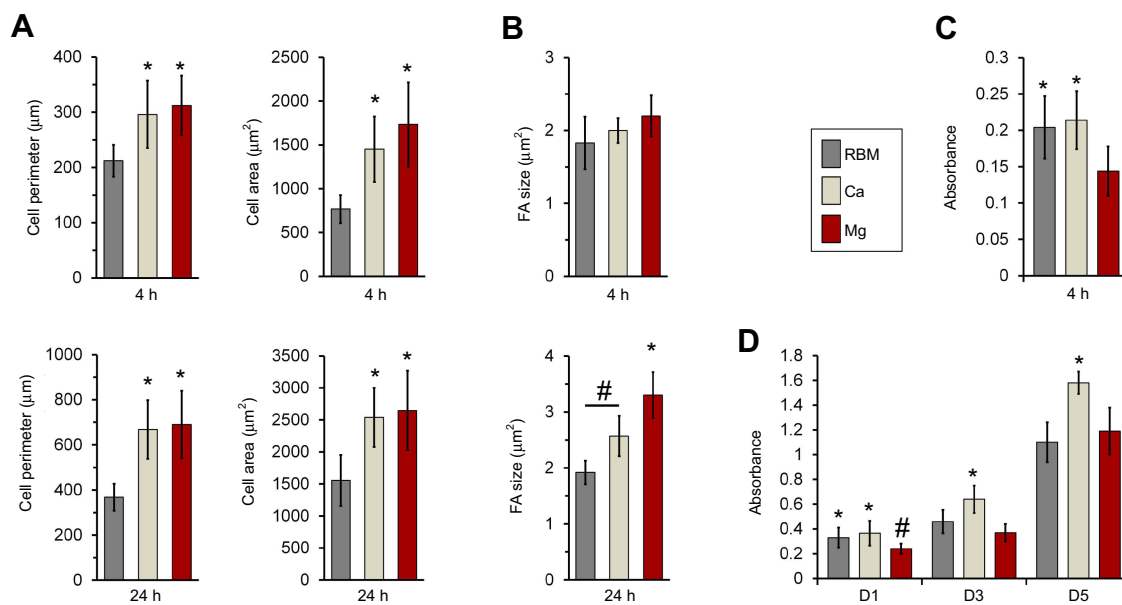


**Figure 8** (A) Quantitative measurements of the cell area and perimeter of the spread mesenchymal stem cells (MSCs) on the investigated surfaces at 4 and 24 hrs of incubation. \* $P<0.05$  compared with the RBM surface. (B) Quantitative measurements of size of focal adhesions in the spread MSCs on the investigated surfaces at 4 and 24 hrs of incubation. \* $P<0.05$  compared with the other surface; # $P<0.05$  between the two surfaces. (C) Early cell attachment expressed by absorbance value (at 4 hrs). \* $P<0.05$  compared with the RBM surface. (D) Cell proliferation (at 1, 3 and 5 days) expressed by the absorbance value. \* $P<0.05$  compared with the other surface; # $P<0.05$  compared to the Mg surface. Values are the mean  $\pm$  SD of three independent experiments.

found in cell proliferation between the RBM and Mg surfaces.

This finding is somewhat in agreement with the results of previous studies reporting increased osteoblast cell proliferation with surface Ca incorporation in the Ti implant surface.<sup>25,26</sup> In contrast, the lower attachment and proliferation with Mg incorporation does not coincide with a previous report.<sup>27</sup> We suppose that these discordant results between the studies are attributable to differences in cell functions between osteoblastic cell lines and primary MSCs employed in our test system. Further, detailed studies are needed to resolve this issue.

## Osteogenic differentiation of the MSCs affected by surface divalent cation modification

After assessing the early cellular events evoked by surface chemistry modification using Ca and Mg ions on a micro-rough Ti implant surface, we investigated the osteogenic potential of modified Ti surfaces. We first evaluated the osteogenic functionality of MSCs by assessing the osteogenesis-related gene expression, ALP activity and type I COL protein production at 7 days of culture.

The expression levels of transcription factors regulating osteogenesis (Dlx5, Runx2 and osterix) in MSCs grown on the investigated samples are shown in Figure 9A. Dlx5 expression was upregulated on the Mg surface compared with the RBM and Ca surfaces ( $P<0.05$ ). Surface Ca and Mg modification notably upregulated gene expression of two critical transcription factors (Runx2 and osterix;  $P<0.05$ ), but expression levels of these two genes in the Ca sample were lower than in the Mg sample ( $P<0.05$ ). Thus, Mg incorporation induced higher mRNA expression of Dlx5, Runx2, and osterix than Ca incorporation when applied to a microrough Ti surface with additional changes in nanotopography.

The mRNA expression levels of the marker genes indicating the stages of early (COL and ALP), intermediate (BSP) and terminal (OC) osteogenic differentiation are shown in Figure 9A. The mRNA expression of the marker genes for osteoblast differentiation exhibited was mostly similar to those of the transcription factor genes (Dlx5, Runx2 and osterix). Surface modification of a microrough Ti sample using Ca and Mg ions upregulated the expression of osteoblast marker genes (COL, ALP, BSP and OC) in primary bone marrow MSCs ( $P<0.05$ ; Figure 9A). Mg ion modification evidently increased COL, ALP and BSP

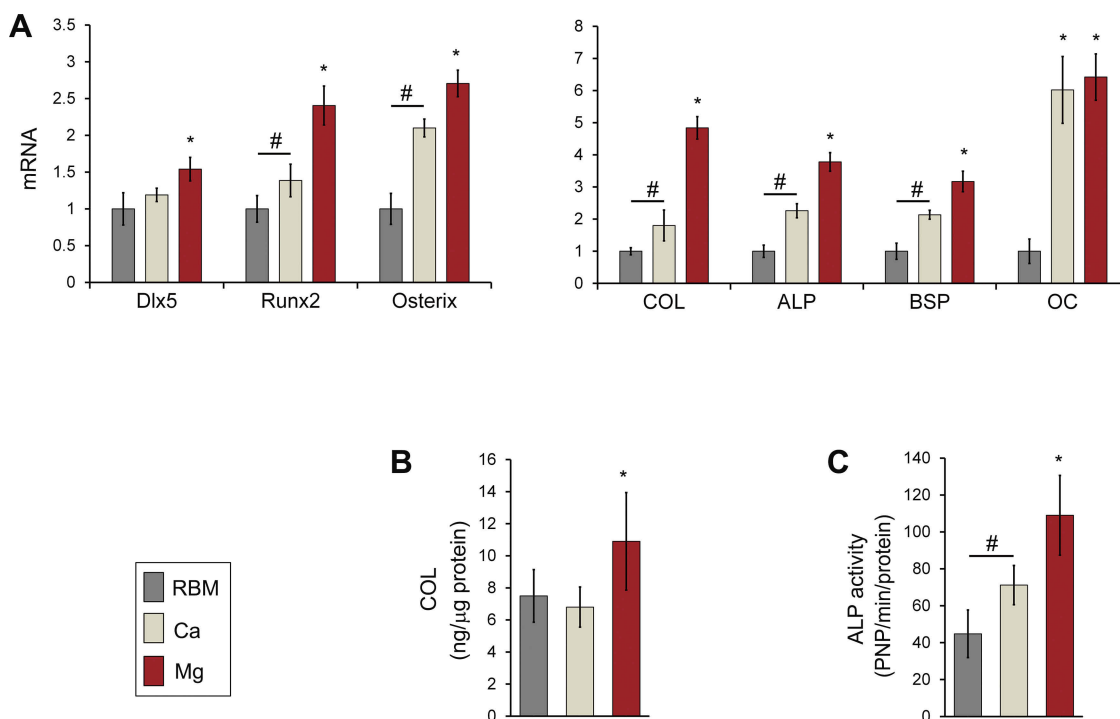


**Figure 9** (A) Quantitative real-time PCR analysis of the mRNA levels of the transcription factor genes for osteogenic differentiation (Dlx5, Runx2 and osterix) and osteoblast phenotype genes (type I collagen [COL], ALP, bone sialoprotein [BSP] and osteocalcin [OC]) at 7 days of culture. \* $P<0.05$  compared with the other surface; # $P<0.05$  between two surfaces. (B) ELISA result for the detection of type I COL protein levels secreted into the cell culture media by MSCs grown on the investigated surfaces after 7 days of incubation. \* $P<0.05$  compared with the other surface. (C) ALP activity of MSCs at 7 days of culture. \* $P<0.05$  compared with the other surface; # $P<0.05$  between the two surfaces. The values are the mean  $\pm$  SD of three independent experiments.

expression more than the Ca ion modification did in the microrough Ti surface ( $P<0.05$ ). OC expression in cells grown on the Ca and Mg surfaces were markedly higher than on the RBM surface (6- to 6.5-fold), but there was no difference in the OC mRNA expression level between the Ca and Mg surfaces.

We then assessed the COL protein secretion level by ELISA. MSCs grown on the Mg surface secreted markedly more COL into the cell culture media compared with the RBM and Ca surfaces ( $P<0.05$ ; Figure 9B). Although the Ca surface displayed increased COL expression at the mRNA level compared with the unmodified RBM surface, there was no difference in COL production at the protein levels between the RBM and Ca surfaces.

ALP activity is an important indicator of early osteoblast differentiation. Cells were grown on the surface of the divalent cations-modified Ti samples (Ca and Mg) exhibited significantly greater ALP activity than those on the RBM sample ( $P<0.05$ ; Figure 9C). Surface Mg modification notably increased ALP activity more than Ca modification did ( $P<0.05$ ; Figure 9C).

Divalent cation incorporation by wet chemical treatment increased the expression of terminal osteogenic markers in MSCs at the protein level (OC and OPG) at 14 days (Figure 10). MSCs grown on the Ca and Mg surfaces secreted significantly higher OC and OPG into cell culture media compared with the RBM surface ( $P<0.05$ ). There was no difference in the OC or OPG production level between the Ca and Mg surfaces.

Studies have demonstrated that surface chemistry modification using bioactive ions, such as Ca and Mg, has the capacity to promote the bone formation of Ti implants by

enhancing early cellular events and subsequent osteogenic differentiation.<sup>2,9,15-17,19,21,26,27</sup> In this study, Ca and Mg-containing nanostructures produced on a microrough Ti implant surface by wet chemical treatment displayed sustained ion release and promoted the osteogenic differentiation of primary MSCs.

In this study, total concentration of Ca ions released from the Ca samples at static and dynamic mode was 7.3 ppm (0.18 mM) and 9.6 ppm (0.24 mM), respectively, with similar Ca concentration showing enhanced osteogenesis capacity reported in another study.<sup>28</sup> Increased Ca concentration by the dissolution of bioactive glass sample (8 ppm = 0.2 mM) enhanced ALP activity and OC expression of osteoblastic MC3T3-E1 cells.<sup>28</sup> Ca ion delivery to a chemically treated nanoporous Ti surface at a very low concentration (approximately at 0.45  $\mu$ M) enhanced OC expression in human bone marrow MSCs.<sup>29</sup> Chitosan-TiO<sub>2</sub> nanotubes scaffolds adsorbed with 0.5 mM CaCl<sub>2</sub> improved proliferation and differentiation of human MG63 cells, in which in vitro biocompatibility of Ti nanotubes scaffolds was improved by Ca ion incorporation in a non-dose dependent manner.<sup>30</sup> In contrast, extracellular Ca<sup>2+</sup> stimulated proliferation and osteogenic differentiation of C3H10T1/2 MSCs in a concentration-dependent manner (1.8–8 mM).<sup>31</sup> Maeno et al reported that low Ca<sup>2+</sup> concentration enhanced cell functions of osteogenic cells.<sup>32</sup> 2–4 mM Ca ion concentration in cell culture medium increased proliferation, OC mRNA expression and matrix mineralization of mouse primary osteoblasts.<sup>32</sup>

In contrast to Ca ions, there are more conflicting results on optimal Mg ion concentration for enhancing the osteogenic function of bone-forming cells.<sup>19-22,33,34</sup> In this

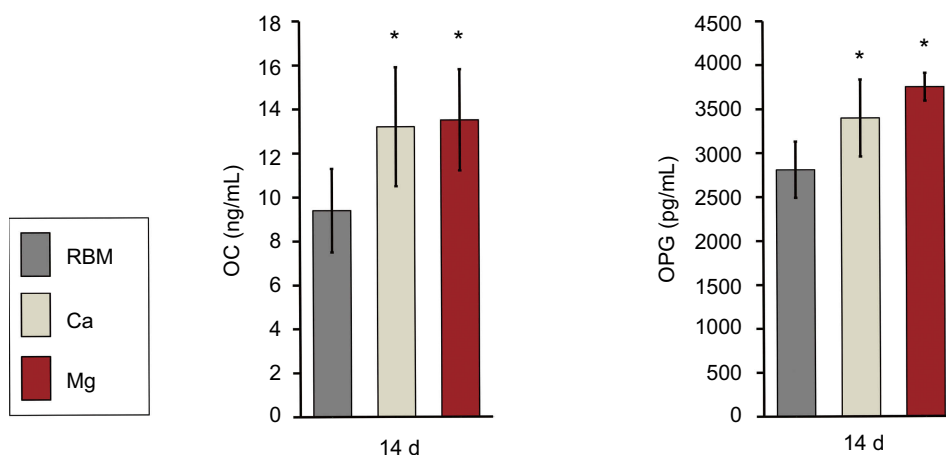


**Figure 10** ELISA results for the detection of the protein levels of terminal osteogenic markers [OC and osteoprotegerin (OPG)] secreted into the culture media by adherent mesenchymal stem cells (MSCs) at 14 days of culture. The values are the mean  $\pm$  SD of three independent experiments. \* $P<0.05$  compared to the RBM surface.

study, the total concentration of Mg ions released from the Mg samples at static and dynamic mode was 1.9 ppm (0.08 mM) and 2.9 ppm (0.12 mM), respectively, which are lower than that reportedly enhanced osteoblast function in other studies.<sup>19–22,33,34</sup> Mg ion supplementation (up to 1.8 mM) dose dependently promoted osteoblast differentiation and mineralization of rabbit bone marrow MSCs.<sup>22</sup> Osteogenic differentiation such as ALP activity, OC gene expression and mineralization was notably increased in primary human osteoblasts with 1 mM and 2 mM Mg ion supplementation, but was markedly impaired with high Mg concentration of 4 mM above.<sup>20</sup> Zhang et al reported that a low Mg concentration (1.3 mM) inhibits matrix mineralization of human bone marrow MSCs.<sup>33</sup> In contrast, 10 mM Mg treatment increased proliferation and matrix mineralization of human bone marrow MSCs.<sup>34</sup> In addition, Mg-based extracts at a high Mg content in culture media (26 mM) enhanced focal adhesion development and osteoblast gene expression of primary human osteoblasts.<sup>21</sup> Although studies have demonstrated that Mg ion supplementation into culture medium and extracts from Mg-based alloys increase osteogenic potential and bone formation, optimal dose of Mg ions and related molecular mechanism for beneficial bone healing effects are still unclear.

It seems that differences of the way of Mg delivery into test system (ie, as culture media supplement and direct incorporation into materials surface) and cell types between studies are possible reasons for the conflicting biologic effect of Mg ions. However, it is worth paying attention to the results of other studies reporting that small deviations of extracellular ion concentrations from physiological value directly controls osteoblast functions.<sup>15,16,35</sup> When considering the concentration of  $\text{Ca}^{2+}$  (1.8 mM) and  $\text{Mg}^{2+}$  (0.8 mM) ions in  $\alpha$ -MEM,<sup>36</sup> we may reasonably suppose that a minute increase of Ca and Mg ion concentration in culture medium through the ion release from the modified Ti surface enhanced osteogenesis-related cell functions of MSCs in this study. However, further detailed studies are needed to clarify this.

It is known that certain external features of implant surface such as surface chemistry, nanotopography and hydrophilicity play critical roles in the regulation of osteogenic cell functions and ultimate implant osseointegration.<sup>1,2,5,8,9,11,17,24–27</sup> Thus, we cannot rule out the contribution of surface nanotopography and wettability in the enhanced osteogenic capacity of the modified Ti implant surface, possibly acting in a synergistic manner.

Thus, it is not possible to determine the precise extent of the effect of ion release solely based on the enhanced osteogenic capacity of the modified Ti implant surface found in this study. Only our supposition is that ionic release from the modified Ti surface increases the extracellular ion concentration in the culture media and this alters the intracellular ion concentration of adherent cells, which consequently activates critical intracellular signaling related to osteogenic differentiation.<sup>15,17,22</sup> In this study, the Mg surface modification exerted a more potent capacity for promoting the osteogenic differentiation of MSCs than the Ca surface modification at the early incubation time-points.

We previously showed that Ca chemistry is a more potent factor than hydrophilicity or nanoscale surface area in promoting early osteogenic differentiation of human MSCs.<sup>9</sup> In addition, a previous study reported that better wettability enhances the early osseointegration of Ti implants having the same bioactive ion chemical composition in rabbit cancellous bone.<sup>37</sup> We suppose that the better wettability of the Mg surface also contributed to the enhanced osteogenic capacity of the Mg surface modification. Thus, it is expected that surface chemistry alteration using Mg ions by wet chemical treatment will prove useful in accelerating early osseointegration of microrough Ti implants at the interface between the bone and implants by enhancing spreading, the development of focal adhesions and the subsequent osteogenic differentiation of MSCs.

These findings indicate that early the osteogenic functionality of bone marrow MSCs may be enhanced by surface modification using Ca- and Mg-containing nanostructures in a clinically available grit-blasted microrough Ti implant surface. More importantly, Mg modification appears to be more potent than Ca modification in promoting early osteogenesis-related cellular functions at least in mouse bone marrow MSCs.

## Total and phosphorylated $\beta$ -catenin protein expression in MSCs induced by Ca and Mg modification

After confirming the relative osteogenic capacity of surface chemistry modification of a microrough Ti implant surface using Ca and Mg ions, we further investigated whether divalent cation chemistry affects  $\beta$ -catenin activity. There are several important signaling networks involved in the regulation of osteogenic differentiation.<sup>38</sup>

It is known that  $\beta$ -catenin activity is essential for osteoblast differentiation and bone formation.<sup>39,40</sup> Inhibition of  $\beta$ -catenin phosphorylation stabilizes intracellular  $\beta$ -catenin.<sup>29,30</sup> It is well known that phosphorylation of  $\beta$ -catenin at the Ser 45 residue triggers subsequent phosphorylation by GSK3 $\beta$  at the Ser 33, Ser 37 and Thr 41 residues,<sup>39</sup> which in turn results in the proteolytic degradation of  $\beta$ -catenin. Accumulation of unphosphorylated  $\beta$ -catenin molecules in the cytoplasm facilitates its translocation into the nucleus. Stabilization of  $\beta$ -catenin is known to positively regulate the osteogenesis-related cell functionality of MSCs by binding to TCF/LEF transcription factors in the nucleus.<sup>41</sup>

The results of semi-quantitative measurement of the protein amount of total cellular  $\beta$ -catenin and phosphorylated  $\beta$ -catenin (pS45) in the cell lysates of MSCs determined by ELISA are shown in Figure 11. At 3 days, there were no differences in the protein levels of the total cellular  $\beta$ -catenin and pS45 in the investigated surfaces. At 7 days, the Mg surface exhibited an increased protein level of total cellular  $\beta$ -catenin compared with the RBM and Ca surfaces ( $P<0.05$ ). Interestingly, surface Mg modification notably decreased  $\beta$ -catenin phosphorylation. The pS45 protein level in MSCs grown on the Mg surface was significantly lower than the RBM and Ca surfaces ( $P<0.05$ ). The Ca surface displayed decreased pS45 protein expression compared with the unmodified RBM surface ( $P<0.05$ ). In

addition, the relative percentage values of the amount of the phosphorylated  $\beta$ -catenin protein in the total amount of cellular  $\beta$ -catenin protein were calculated. There was no difference in the relative percentage values of pS45/total  $\beta$ -catenin between the RBM and Ca surfaces. The Mg surface exhibited a significantly lower value in the relative percentage of pS45/total  $\beta$ -catenin compared with the RBM and Ca surfaces at 7 days ( $P<0.05$ ; Figure 11).

These findings indicate that surface Mg modification inhibits  $\beta$ -catenin phosphorylation. Consequently, an increased amount of unphosphorylated  $\beta$ -catenin accumulated in the cytoplasm of MSCs would be expected to subsequently increase the translocation of  $\beta$ -catenin into the nucleus, which in turn would trigger certain osteogenesis-related intracellular signaling cascades. Thus, the stabilization of  $\beta$ -catenin appears to be one of the critical mechanisms underlying the enhanced osteogenic capacity of the surface Mg incorporation observed in this study.

## Conclusion

This study evaluated which of the divalent cations examined in this study, Ca or Mg, plays the more dominant role in the early osteogenic functionality of MSCs when employed in the surface chemistry modification of microstructured Ti implants. In this study, Ca- and Mg-containing nanostructures produced by a wet chemical treatment enhanced early spreading, the development of

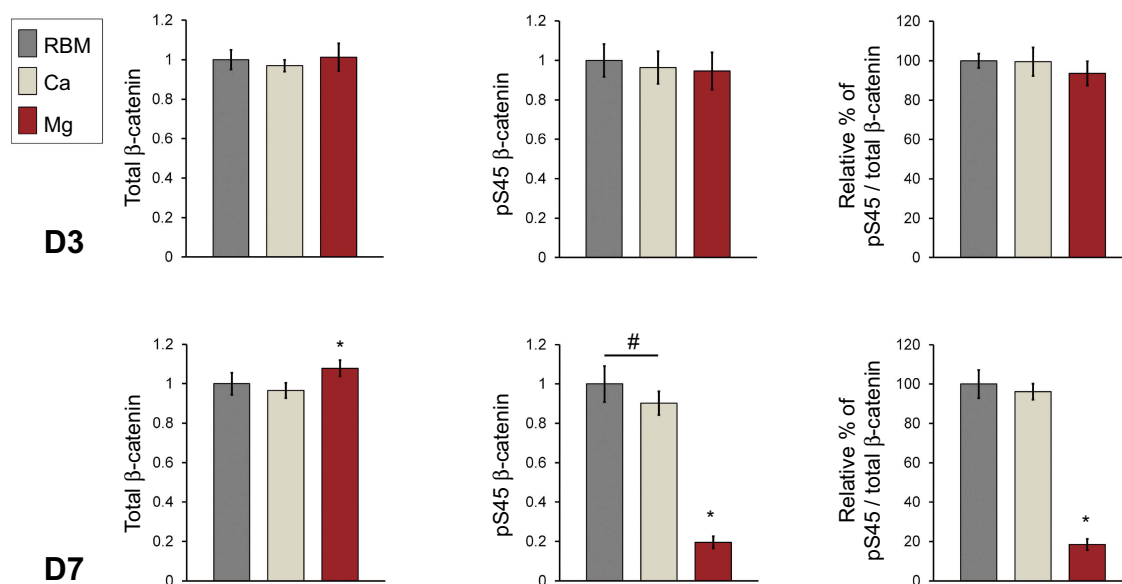


**Figure 11** ELISA results for the detection of the protein expression levels of total cellular  $\beta$ -catenin, phosphorylated  $\beta$ -catenin (pS45), and the relative percentage of phosphorylated  $\beta$ -catenin (pS45) in the total cellular  $\beta$ -catenin (expressed as a percentage of the unmodified RBM surface) in the cell lysate of MSCs adhering to the investigated samples at 3 and 7 days of culture. The values are the mean  $\pm$  SD of three independent experiments. \* $P<0.05$  compared with the other surface; # $P<0.05$  between the two surfaces.

focal adhesions and the subsequent osteogenic differentiation of primary bone marrow MSCs in microrough Ti implant surface. Surface Mg modification exhibited a more potent capacity in promoting early osteogenic differentiation of MSCs than the Ca modification. It is expected that a Mg-containing surface nanostructure with its better wettability would be more beneficial for driving the early osteogenic differentiation of MSCs in a microrough Ti implant surface by enhancing spreading, focal adhesion formation and stabilization of intracellular  $\beta$ -catenin when compared with a Ca-containing nanostructure with its lower surface wettability.

## Acknowledgments

This research was supported by the Basic Science Research Program through the National Research Foundation of Korea (NRF) funded by the Korean government (NRF-2017R1A2A2A05001442).

## Disclosure

The authors report no conflicts of interest in this work.

## References

- Ma QL, Zhao LZ, Liu RR, et al. Improved implant osseointegration of a nanostructured titanium surface via mediation of macrophage polarization. *Biomaterials*. 2014;35:9853–9867. doi:10.1016/j.biomaterials.2014.08.025
- Wang G, Li J, Zhang W, et al. Magnesium ion implantation on a micro/nanostructured titanium surface promotes its bioactivity and osteogenic differentiation function. *Int J Nanomed*. 2014;9:2387–2398.
- Gastaldi G, Grusovin MG, Felice P, Barausse C, Ippolito DR, Esposito M. Early loading of maxillary titanium implants with a nanostructured calcium-incorporated surface (Xpeed): 5-year results from a multi-centre randomized controlled trial. *Eur J Oral Implantol*. 2017;10:415–424.
- Offermanns V, Andersen OZ, Sillassen M, et al. A comparative in vivo study of strontium-functionalized and SLActive™ implant surfaces in early bone healing. *Int J Nanomed*. 2018;13:2189–2197. doi:10.2147/IJN.S177627
- Choi SM, Park JW. Multifunctional effects of a modification of SLA titanium implant surface with strontium-containing nanostructures on immunoinflammatory and osteogenic cell function. *J Biomed Mater Res A*. 2018;106:3009–3020. doi:10.1002/jbm.a.36490
- Sul YT, Kwon DH, Kang BS, Oh SJ, Johansson C. Experimental evidence for interfacial biochemical bonding in osseointegrated titanium implants. *Clin Oral Implants Res*. 2013;A100(Suppl):8–19. doi:10.1111/j.1600-0501.2011.02355.x
- Park JW, Koh HJ, Jang JH, Kang H, Suh JY. Increased new bone formation with a surface magnesium-incorporated deproteinized porcine bone substitute in rabbit calvarial defects. *J Biomed Mater Res A*. 2012;100:834–840. doi:10.1002/jbm.a.34017
- Li Z, Gao P, Wan P, et al. Novel bio-functional magnesium coating on porous Ti6Al4V orthopaedic implants: in vitro and in vivo study. *Sci Rep*. 2017;7:40755. doi:10.1038/srep40755
- Kim HS, Kim YJ, Jang JH, Park JW. Surface engineering of nanostructured titanium implants with bioactive ions. *J Dent Res*. 2016;95:558–565. doi:10.1177/0022034516638026
- Park JW, An CH, Jeong SH, Suh JY. Osseointegration of commercial microstructured titanium implants incorporating magnesium: a histomorphometric study in rabbit cancellous bone. *Clin Oral Implants Res*. 2012;23:294–300. doi:10.1111/j.1600-0501.2010.02144.x
- Park JW, Kim YJ, Park CH, et al. Enhanced osteoblast response to an equal channel angular pressing-processed pure titanium substrate with microrough surface topography. *Acta Biomater*. 2009;5:3272–3280. doi:10.1016/j.actbio.2009.04.029
- Humphries JD, Wang P, Streuli C, Geiger B, Humphries MJ, Ballestrem C. Vinculin controls focal adhesion formation by direct interactions with talin and actin. *J Cell Biol*. 2007;179:1043–1057. doi:10.1083/jcb.200703036
- Kim DH, Wirtz D. Focal adhesion size uniquely predicts cell migration. *FASEB J*. 2013;27:1351–1361. doi:10.1096/fj.12-216564
- Komasa S, Kusumoto T, Taguchi Y, et al. Effect of nanosheet surface structure of titanium alloys on cell differentiation. *J Nanomater*. 2014;2014:642527.
- Dvorak MM, Siddiqua A, Ward DT, et al. Physiological changes in extracellular calcium concentration directly control osteoblast function in the absence of calciotropic hormones. *Proc Natl Acad Sci U S A*. 2004;101:5140–5145. doi:10.1073/pnas.0306141101
- Gustavsson J, Ginebra MP, Planell J, Engel E. Osteoblast-like cellular response to dynamic changes in the ionic extracellular environment produced by calcium-deficient hydroxyapatite. *J Mater Sci Mater Med*. 2012;23:2509–2520. doi:10.1007/s10856-012-4705-4
- Barradas AM, Fernandes HA, Groen N, et al. A calcium-induced signaling cascade leading to osteogenic differentiation of human bone marrow-derived mesenchymal stromal cells. *Biomaterials*. 2012;33:3205–3215. doi:10.1016/j.biomaterials.2012.01.020
- Krebs J, Agellon LB, Michalak M. Ca<sup>2+</sup> homeostasis and endoplasmic reticulum (ER) stress: an integrated view of calcium signaling. *Biochem Biophys Res Commun*. 2015;460:114–121. doi:10.1016/j.bbrc.2015.02.004
- Zhang Z, Zu H, Zhao D, et al. Ion channel functional protein kinase TRPM7 regulates Mg ions to promote the osteoinduction of human osteoblast via PI3K pathway: in vitro stimulation of the bone-repairing effect of Mg-based alloy implant. *Acta Biomater*. 2017;63:369–382. doi:10.1016/j.actbio.2017.08.051
- Wang J, Ma XY, Feng YF, et al. Magnesium ions promotes the biological behavior of rat calvarial osteoblasts by activating the PI3K/Akt signaling pathway. *Biol Trace Elem Res*. 2017;179:284–293. doi:10.1007/s12011-017-0948-8
- Burmester A, Willumeit-Romer R, Feyerabend F. Behavior of bone cells in contact with magnesium implant material. *J Biomed Mater Res Part B*. 2017;105:165–179. doi:10.1002/jbm.b.33542
- Diaz-Tocados JM, Herencia C, Martinez-Moreno JM, et al. Magnesium chloride promotes osteogenesis through notch signaling activation and expansion of mesenchymal stem cells. *Sci Rep*. 2017;7:7839. doi:10.1038/s41598-017-08379-y
- Mathieu PS, Lobo EG. Cytoskeletal and focal adhesion influences on mesenchymal stem cell shape, mechanical properties, and differentiation down osteogenic, adipogenic, and chondrogenic pathways. *Tissue Eng Part B Rev*. 2012;18:436–444. doi:10.1089/ten.teb.2012.0014
- Yang J, McNamara LE, Gadegaard N, et al. Nanotopographical induction of osteogenesis through adhesion, bone morphogenic protein cosignaling, and regulation of microRNAs. *ACS Nano*. 2014;8:9941–9953. doi:10.1021/nn504767g
- Park JW, Suh JY, Chung HJ. Effects of calcium ion incorporation on osteoblast gene expression in MC3T3-E1 cells cultured on microstructured titanium surfaces. *J Biomed Mater Res A*. 2008;86:117–126. doi:10.1002/jbm.a.31595

26. Park JW, Tustusmi Y, Lee CS, et al. Surface structures and osteoblast response of hydrothermally produced CaTiO<sub>3</sub> thin film on Ti-13Nb-13Zr alloy. *Appl Surf Sci.* 2011;257:7856–7863. doi:10.1016/j.apsusc.2011.04.054
27. Park JW, Kim YJ, Jang JH, Song H. Osteoblast response to magnesium ion-incorporated nanoporous titanium oxide surfaces. *Clin Oral Implants Res.* 2010;21:1278–1287. doi:10.1111/j.1600-0501.2010.01944.x
28. Varanasi VG, Saiz E, Loomer PM, et al. Enhanced osteocalcin expression by osteoblast-like cells (MC3T3-E1) exposed to bioactive coating glass (SiO<sub>2</sub>-CaO-P<sub>2</sub>O<sub>5</sub>-MgO-K<sub>2</sub>O-Na<sub>2</sub>O system) ions. *Acta Biomater.* 2009;5:3536–3547. doi:10.1016/j.actbio.2009.04.029
29. Sawada R, Kono K, Isama K, Haishima Y, Matsuoka A. Calcium-incorporated titanium surfaces influence the osteogenic differentiation of human mesenchymal stem cell. *J Biomed Mater Res A.* 2013;101:2573–2585. doi:10.1002/jbm.a.34566
30. Lim SS, Chai CY, Loh HS. In vitro evaluation of osteoblast adhesion, proliferation and differentiation on chitosan-TiO<sub>2</sub> scaffolds with Ca<sup>2+</sup> ions. *Mater Sci Eng C Mater Biol Appl.* 2017;76:144–152. doi:10.1016/j.msec.2017.03.075
31. Lee MN, Hwang HS, Oh SH, et al. Elevated extracellular calcium ions promote proliferation and migration of mesenchymal stem cells via increasing osteopontin expression. *Exp Mol Med.* 2018;50:142. doi:10.1038/s12276-018-0170-6
32. Maeno S, Niki Y, Matsumoto H, et al. The effect of calcium ion concentration on osteoblast viability, proliferation and differentiation in monolayer and 3D culture. *Biomaterials.* 2005;26:4847–4855. doi:10.1016/j.biomaterials.2005.01.006
33. Zhang L, Yang C, Li J, Zhu Y, Zhang X. High extracellular magnesium inhibits mineralized matrix deposition and modulates intracellular calcium signaling in human bone marrow-derived mesenchymal stem cells. *Biochem Biophys Res Commun.* 2014;450:1390–1395. doi:10.1016/j.bbrc.2014.05.144
34. Yoshizawa S, Brown A, Barchowsky A, Sfeir C. Magnesium ion stimulation of bone marrow stromal cells enhances osteogenic activity, stimulating the effect of magnesium alloy degradation. *Acta Biomater.* 2014;10:2834–2842. doi:10.1016/j.actbio.2014.02.002
35. Habel B, Glaser R. Human osteoblast-like cells respond not only to the extracellular calcium concentration but also to its change rate. *Eur Biophys J.* 1998;27:411–416. doi:10.1007/s002490050149
36. Kruppke B, Heinemann C, Wagner AS, et al. Strontium ions promote in vitro human bone marrow stromal cell proliferation and differentiation in calcium-lacking media. *Dev Growth Differ.* 2019;61:166–175. doi:10.1111/dgd.12588
37. Park JW. Osseointegration of two different phosphate ion-containing titanium oxide surfaces in rabbit cancellous bone. *Clin Oral Implants Res.* 2013;100(SA):145–151. doi:10.1111/j.1600-0501.2011.02406.x
38. Soltanoff CS, Chen W, Yang S, Li YP. Signaling networks that control the lineage commitment and differentiation of bone cells. *Crit Rev Eukaryot Gene Expr.* 2009;19:1–46. doi:10.1615/CritRevEukaryotGeneExpr.v19.i1.10
39. Song L, Liu M, Ono N, Bringhurst FR, Kronenberg HM, Guo J. Loss of wnt/β-catenin signaling causes cell fate shift of preosteoblasts from osteoblasts to adipocytes. *J Bone Miner Res.* 2012;27:2344–2358. doi:10.1002/jbmr.v27.11
40. Amit S, Hatzubai A, Birman Y, et al. Axin-mediated CKI phosphorylation of beta-catenin at Ser 45: a molecular switch for the Wnt pathway. *Genes Dev.* 2002;16:1066–1076. doi:10.1101/gad.979902
41. Galli C, Piemontese M, Lumetti S, Manfredi E, Macaluso GM, Passeri G. The importance of WNT pathways for bone metabolism and their regulation by implant topography. *Eur Cell Mater.* 2012;24:46–59. doi:10.22203/eCM.v024a04

## International Journal of Nanomedicine

### Publish your work in this journal

The International Journal of Nanomedicine is an international, peer-reviewed journal focusing on the application of nanotechnology in diagnostics, therapeutics, and drug delivery systems throughout the biomedical field. This journal is indexed on PubMed Central, MedLine, CAS, SciSearch®, Current Contents®/Clinical Medicine,

Submit your manuscript here: <https://www.dovepress.com/international-journal-of-nanomedicine-journal>

Dovepress

Journal Citation Reports/Science Edition, EMBase, Scopus and the Elsevier Bibliographic databases. The manuscript management system is completely online and includes a very quick and fair peer-review system, which is all easy to use. Visit <http://www.dovepress.com/testimonials.php> to read real quotes from published authors.